THE ASTROPHYSICAL JOURNAL, 315:687–699, 1987 April 15

EINSTEIN OBSERVATORY SURVEY OF X-RAY EMISSION FROM SOLAR-TYPE STARS: THE LATE F AND G DWARF STARS

A. MAGGIO,[1] S. SCIORTINO,[1] G. S. VAIANA,[1,2] P. MAJER,[2,3] J. BOOKBINDER,[2] L. GOLUB,[2] F. R. HARNDEN,[2] JR., AND R. ROSNER[2]

Received 1986 March 13; accepted 1986 October 1

ABSTRACT

We present results of a volume-limited X-ray survey of stars of luminosity classes IV and V in the spectral range F7–G9 observed with the *Einstein Observatory*. Only stars without any peculiarities in their optical spectrum were included in our sample. Using survival analysis techniques, we derive the stellar X-ray luminosity function in the 0.15–4.0 keV energy band for both single and multiple sources. We show that the difference in X-ray luminosity between these two classes of sources is consistent with the superposition of individual components in multiple-component systems, whose X-ray properties are similar to those of the single-component sources. The X-ray emission of the stars in our sample is well correlated with their chromospheric Ca II H-K line emission and with their projected equatorial rotational velocity (or, alternatively, with their Rossby number). Comparison of the X-ray luminosity function constructed for the sample of the dG stars of the local population with the corresponding functions derived elsewhere for the Hyades, the Pleiades, and the Orion Ic open cluster confirms that the level of X-ray emission decreases with stellar age.

Subject headings: Ca II emission — stars: evolution — stars: X-rays

I. INTRODUCTION

The aim of the early *Einstein Observatory* surveys of stellar X-ray emission (Vaiana *et al.* 1981; Helfand and Caillault 1982; Topka *et al.* 1982) was to assess the pervasiveness of stellar X-ray emission and to describe the general behavior of this emission throughout the H-R diagram. As a result of these initial studies, we learned that classical stellar parameters such as the color index, absolute visual magnitude, and surface gravity are not indicators of the X-ray emission level of normal stars. From solar observations, we know that magnetic-related phenomena largely determine the level of solar coronal activity, and hence of solar X-ray emission; arguing by analogy, we expect the same to hold for solar-type stars (Vaiana and Rosner 1978; Golub 1982; Vaiana 1983). Since the surface magnetic activity level is presumably governed by the emergence rate of magnetic fields from the stellar interior, and hence by magnetic dynamo processes (cf. Parker 1979), we expect that the stellar parameters governing dynamo activity are also important in determining X-ray activity levels. Hence, such parameters as rotation rate probably influence the level of X-ray emission in normal late-type stars (although quantitative theoretical predictions still elude us; cf. Rosner 1983). It then remains to establish the observational relation between the level of stellar X-ray emission and these magnetic dynamo–related stellar parameters.

With this concern in mind, we have carried out a statistically complete survey of X-ray emission from late F and G dwarf stars in the solar neighborhood. This work is part of our ongoing study of X-ray properties of normal dwarf stars using data from the *Einstein Observatory*, including X-ray surveys of A stars (Golub *et al.* 1983), main-sequence stars with shallow convection zones (Schmitt *et al.* 1985*a*), low-mass stars (Rosner *et al.* 1981; Bookbinder 1985), and open cluster stars in the Hyades (Micela *et al.* 1987), the Pleiades (Micela *et al.* 1985), and Ursa Major (Walter *et al.* 1984); and complement surveys of normal stars carried out by others using *Einstein Observatory* data (for example, see Stern *et al.* 1981; Walter 1981, 1982, 1983; Johnson 1983; Caillault and Helfand 1985).

This paper is organized as follows: in § II we describe the procedures and criteria used to select our star sample; data reduction is discussed in § III. The statistical analysis of the data and its implications are discussed in § IV, and our results are summarized in § V.

II. SURVEY COMPOSITION

a) Sample Selection

Our sample has been selected from all stars of luminosity classes IV and V which lie in the spectral type range F7–G9, are located within a distance of 25 pc, and fell into one of the *Einstein Observatory* imaging proportional counter (IPC) fields of view. The bulk of the optical parent sample has been extracted from the Woolley catalog (Woolley *et al.* 1970), but a few sources have been added from the addendum list to the Gliese catalog (Gliese and Jahreiss 1979), from which we also adopted all improvements (or corrections) to stellar distances. The choice of the distance cutoff of 25 pc was motivated by the conflicting needs of obtaining as large a sample as possible, yet one which is also homogeneous and well characterized (including spectral type, distance, multiplicity, and possible spectral or elemental peculiarities). This led to an initial sample of 401 stars.

For the sake of homogeneity, we have eliminated from this optical "parent" sample the three "certain" Pleiades members (as suggested by Gliese 1969), because they are likely to be more distant than 25 pc. We then selected all stars from this optical parent sample which fell either serendipitously or as targets in *Einstein* IPC fields, The resulting sample consists of 69 stars, so that $\sim 18\%$ of the optical candidates satisfying the prescribed requirements have been observed by the *Einstein Observatory*. Finally, we have rejected five certain or

[1] Osservatorio Astronomico di Palermo, Italy.
[2] Harvard-Smithsonian Center for Astrophysics.
[3] Wroclaw Astronomical Observatory, Poland.

TABLE 1

Optical Properties of the Sample Stars

Star Name	HD/BD	Hoffleit and Jaschek 1982	Other Name	Sp[a]	M_v	$B-V$	Distance (pc)	Remarks[a]
Sun	…	…	…	G2 V	4.71	0.66	…	Not directly observed[b]
W17	1581	77	ζ Tuc	F9 V	4.95	0.58	7.19	
W9012	1835	88	9 Cet	G2 V	4.84	0.66	20.41	Cp at 202″.1, Hyades group
W34AB	4614	219	η Cas	G3 V + K4 Ve	4.60	0.58	5.85	8 components, optical SB1O AB: 11″.994
W9032	5294	…	…	G5 IV	5.85	0.65	20.41	
W0935	5817	…	…	G2 V	6.41	0.64	25.00	
W71	10700	509	τ Cet	G8 V	5.71	0.72	3.61	Cp at 89″.8
W9073AB	13043	…	…	G2 V + dK	4.91	0.62	25.00	CP at 84″
W9085	16141	…	79 Cet	G5 IV	4.88	0.67	24.39	
W9092A	16619	…	…	G4 V	6.00	0.65	23.26	Ca II in emission, Cp at 0″.148
W9095	16739	788	12 Per	F9 V	2.94	0.58	25.00	SB2O Cp at 0″.053
W124	19373	937	ι Per	G0 V	3.72	0.60	11.63	Cp at 146″.2
W137	20630	996	κ Cet	G5 Vv	4.97	0.68	9.43	Ca II emission, triple system AB:268″.7, AC:251″
W139	20794	1008	82 Eri	G5 V	5.29	0.71	6.21	Also G8 III
W147	22484	1101	10 Tau	F9 V	3.21	0.57	16.39	Cp at 396″ CPM?
W160	25680	1262	39 Tau	G5 V	5.09	0.62	14.49	Triple system, AB:170″.1
W9177	33811	…	…	G5	6.72	0.77	25.00	
W202	35296	1780	111 Tau	F8 V	4.01	0.53	15.87	Ca II in emission, SB, optical Cp at 85″.7
W209	37124	…	…	G4 V	6.31	0.67	18.18	
W222	39587	2047	χ^1 Ori	G0 V	4.45	0.59	9.80	Triple system?. SB?, Cp at 0″.6 U Ma stream member
W9205	42250	…	…	G7 V	5.60	0.77	23.26	
W9209AB	44120	…	…	G3 V + F8 V	4.56	0.59	23.81	Triple system, AB:38″.3
W291	64096	3064	9 Pup	F9 V + G4 V	4.22	0.60	15.39	SBO AB:0″.580, U Ma stream member?
W311	72905	3391	π^1 UMa	G1.5 Vb	4.83	0.62	14.49	U Ma stream member
W327	76151	3538	…	G3 V	5.65	0.67	11.77	
W9286	78418	3626	75 Cnc	G5 IV–V	4.12	0.65	23.81	Triple system, SB20, Cp at 112″
W364	84117	3862	…	F9 IV	4.42	0.53	12.66	
W368	84737	3881	15 LMi	G0.5 Va	4.20	0.62	15.15	
W9322	88725	…	…	G1 V	5.93	0.60	23.26	
W384A	88746	…	…	G8 V	7.22	0.79	15.15	Cp at $\sim 5''$, $m_v(B) = 10.8$
W395	90839	4112	36 UMa	F8 V + K7 V	4.27	0.52	12.99	Triple CPM, RV system, AC: 139″
W417	97334	4345	…	G0 V	4.53	0.61	23.81	4 components AB: 138″.7
W9357	98281	…	…	G8 V	5.96	0.73	18.52	
W434	101501	4496	61 UMa	G8 V	5.77	0.74	8.20	Cp at 159″.3
W449	102870	4540	β Vir	F9 V	3.60	0.55	10.00	Triple system, BC optical, AC:512″.3
GJ 1152	+35 2288	…	…	G7 IV	7.91	0.78	22.22	
W475	109358	4785	β CVn	G0 V	4.46	0.59	9.17	SB1O
W502	114710	4983	β Com	G0 V	4.66	0.58	8.33	SB?, Cp at 90″.8
W504	115383	5011	59 Vir	G0 Vs	4.65	0.58	12.99	Cp at 34″.3, $m_v = 14.3$
W534	121370	5235	η Boo	G0 IV	2.72	0.58	9.80	Triple system?, SB1O AB:112″.6, B is 8.8v
W547	126053	5384	…	G1 V	5.20	0.63	16.39	
W559A	128620	5459	α^1 Cen	G2 V	4.37	0.68	1.33	Triple system, C at 2°.2 CPM SBO AB:20″.9, B:K0 V
W561	…	…	…	G5	8.08	0.68	19.23	
W584AB	137107/8	5527/8	η CrB	G0 V + G3 V	3.91	0.58	16.39	4 components, SBO, AB:0″.839 C at 58″, D at 215″
W598	141004	5868	λ Ser	G0 V	4.30	0.60	10.64	SB1O
W9537	143761	5968	ρ CrB	G2 V	3.54	0.60	23.81	Cp optical at 89″.6
W9538	144284	5986	τ Dra	F8 IV	2.34	0.52	21.74	SB1O $a \sin i = 1''.07$
W9543	144287	…	…	G8 V	5.72	0.77	18.87	SB
W9583	154417	6349	…	F8.5 IV–V	4.46	0.57	20.41	
W666AB	156274	6416	…	G8 V + M0 V	6.07	0.80	7.63	4 components C at 42″, D at at 47″ AB:8″.826
W672	157214	6458	72 Her	G0 V	4.71	0.62	13.70	Triple system SB? AB:230″ B optical not CPM
W684AB	160269	6573	26 Dra	G0 Va + K3 V	4.39	0.61	14.71	Triple system, AB:1″.52, C (dM1) at 740″ CPM
W695ABC	161797	6623	μ Her	G5 IV + 2(dM4)	3.96	0.75	7.81	BC: Ca II in emission, 4 components AXBC:33″.8

TABLE 1—*Continued*

Star Name	HD/BD	Hoffleit and Jaschek 1982	Other Name	Sp[a]	M_v	$B-V$	Distance (pc)	Remarks[a]
W746	178428	7260	...	G5 V	4.93	0.70	16.95	SBO Cp at 21″.5
W9658	183650	...	...	G5 V	5.42	0.72	20.41	
W779	190406	7672	15 Sge	G1 V	4.62	0.61	17.24	6 components AC:203″.7
W780	190248	7665	δ Pav	G6–8 IV	4.78	0.76	5.71	Metal-rich star with normal Doppler broadening
W9685	190771	7683	...	G5 IV	4.37	0.64	22.73	Triple system AC:40″, B at 12″.4, optical 13.2v
W9751	206860	8314	...	G0 V	5.10	0.58	15.15	Active chromosphere star, Var due to starspots?
W882	217014	8729	51 Peg	G2.5 IVa	4.82	0.67	13.70	Also G5 V
W9812AB	218641/0	...	...	G2 V + A2	2.69	0.65	25.00	Cp at 0″.4
W904	222368	8969	ι Psc	F7 V	3.39	0.51	14.09	Optical Cp at 69″.9

[a] Spectral classes and most of the remarks from Hoffleit and Jaschek 1982. "SB1" and "SB2" indicate spectroscopic binaries with single or double lined spectra respectively; the further suffix O signifies that an orbit has been determined. "Cp," companion; "CPM," common proper motion; "RV," radial velocity; letters A, B, C, indicate the brightest members in the multiple systems

[b] Cf. Schmitt *et al.* 1986 for inferences of solar X-ray emission from *Einstein* observations of the sunlit Earth.

"suspected" RS CVn–type stars (from lists of Hall 1981; Basri, Laurent, and Walter 1983; and Eker 1985), one star with a suspected accreting companion (whose X-ray emission would presumably not be of stellar coronal origin), and two stars with peculiar spectra or anomalous metal abundances (because X-ray fluxes are computed on the assumption of thermal emission from a plasma with solar abundances).

Our final sample consists of 61 stars, which are listed in Table 1 together with relevant optical properties. An H-R diagram of the stars in our sample and their distribution as a function of $B-V$ color are shown in Figure 1. About half of all the final sample stars are in multiple systems, so that the possibility of multiple X-ray components must be accounted for (see § IV); we do not know the spectral type of at least one of the secondary components for 28 of these 31 systems, but among the 11 F7–G9 sources with at least one classified companion, that component is typically later than K0.

b) Comparison of Optical Parent and Final X-Ray Selected Samples

Because about half our X-ray data derive from pointed observation, it is necessary to test whether our sample is representative of the nearby star population. We therefore constructed integral distribution functions for the color index $B-V$ (Fig. 2*a*), absolute V-magnitude M_v (Fig. 2*b*), and distance D (Fig. 2*c*) for both the optically selected parent sample and the final X-ray selected sample. Using nonparametric two-sample tests (Schmitt 1985), we tested the null hypothesis that the optical parent sample and the *Einstein Observatory* subsample are drawn from the same parent population, using each one of the above parameters ($B-V$, M_v, D) in turn. We find that we can accept the null hypothesis that the two samples are drawn from the same distribution at the 3 σ confidence level for $B-V$ and M_v but reject it at the same level for distance, indicating that the spectral class coverage of our final sample is reasonably complete, but that the sample's distance coverage, i.e., volume coverage, is relatively poor. Indeed, an inspection of Figure 2*c* shows that we miss a large number of objects whose distances are 15 pc or greater, a result which is consistent with the large number of pointed observations in the X-ray selected sample. To clarify the bias of our X-ray selected sample, we construct the integral distribution function for stellar distance for two distinct subsamples, namely (1) all stars whose distance is less than 10 pc and (2) all stars whose distance lies between 10 and 25 pc, for both the optical parent sample and the X-ray selected sample. The resulting integral

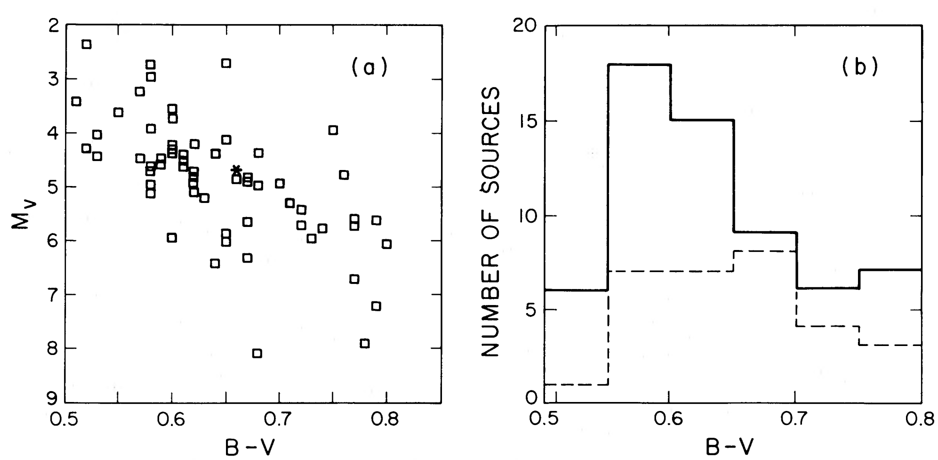

FIG. 1.—(*a*) H-R diagram of the optical candidates in our full survey sample. The Sun position is indicated by an asterisk. (*b*) Distribution of the sample stars as a function of $B-V$ color. *Solid line*, total sample; *dashed line*, single stars.

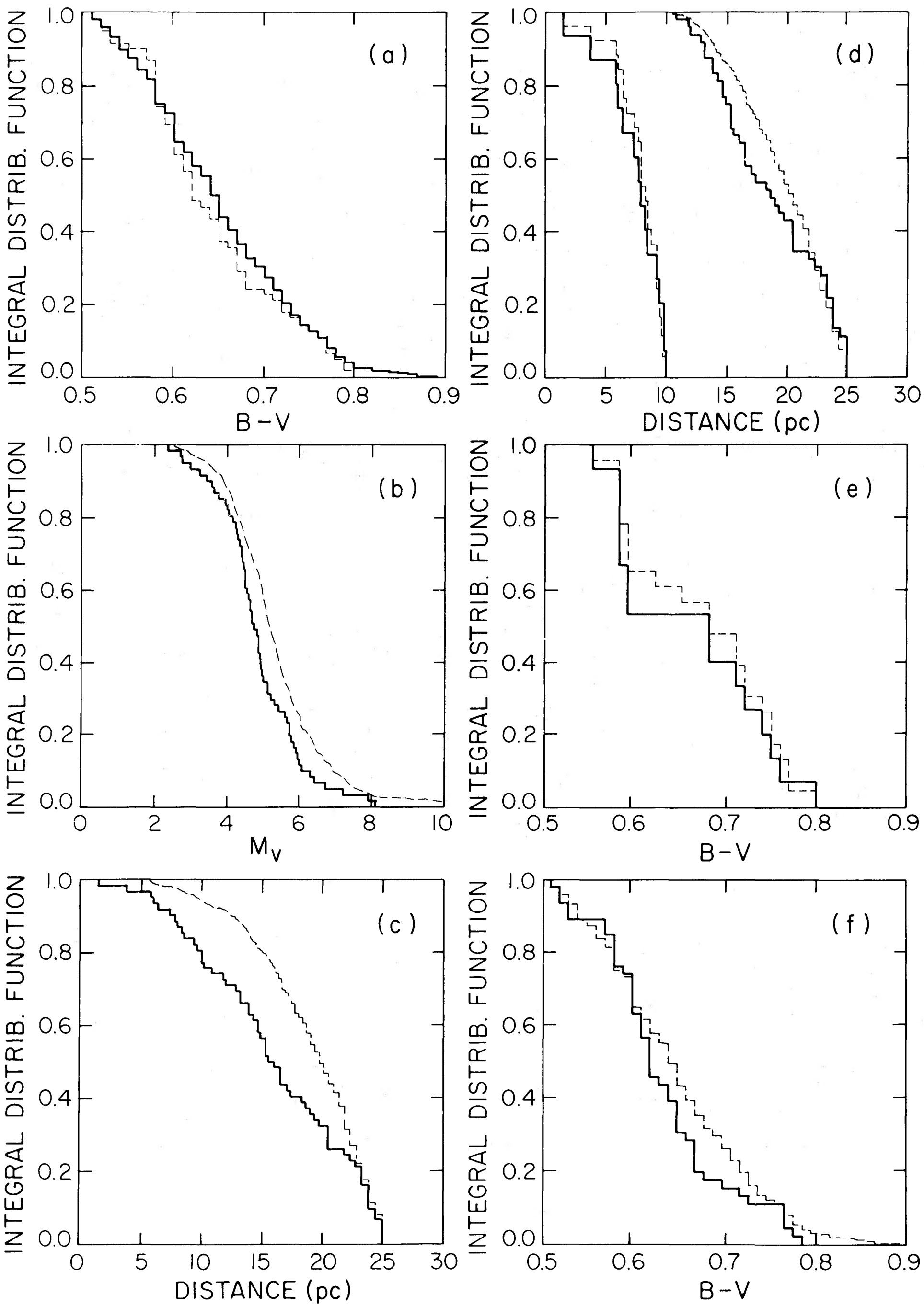

FIG. 2.—(*a*) Integral distribution functions for the $B-V$ color: *solid line*, full sample; *dashed line*, optical parent sample. (*b*) Same, for absolute visual magnitude. (*c*) Same for source distance. (*d*) Integral distribution functions for the distance of stars within 10 pc (*left*) and between 10 and 25 pc (*right*). *Solid lines* survey sample; *dashed lines* optical parent sample. (*e*) Integral distribution functions for the $B-V$ color for stars within 10 pc: *solid line*, survey stars; *dashed line*, optical parent sample. (*f*) Same, for stars between 10 and 25 pc.

distribution functions are shown in Figure 2*d*. Note that although the integral distribution functions of the two subsamples of stars within 10 pc are essentially indistinguishable, the integral distribution functions of the two subsamples whose distance lies between 10 and 25 pc are not, and instead resemble the integral distribution functions of the two full samples (e.g., Fig. 2*c*). This effect occurs because the nearby sample is more complete: we observe $\sim$60% of the nearby sample (25 optical candidates) in X-rays, but only $\sim$12.5% of the larger distant optical sample (376 optical candidates). However, the resulting bias is not strong, because the distribution of $B-V$, shown in Figures 2*e* and 2*f*, is essentially the same for the optical parent sample and the X-ray selected sample in both the distance ranges we consider. That is, although our final sample is not uniformly distributed in space, it is an unbiased sample in its color distribution.

A further comment is needed about the slight (statistically insignificant) difference seen in Figure 2*b* between the M_v distributions of the optical and X-ray samples. It is obvious that the optical sample has an excess of low-luminosity stars: in fact, $\sim 2\%$ of the optical candidates have $M_v \gtrsim 8$ mag, while none are present in the final X-ray sample. The spectral classification of these faint stars is not very precise: most of them lack both luminosity class and $B-V$ color information in the Woolley catalog. We suspect that these stars are subdwarfs which were spuriously included in the optical sample, but in the absence of definitive optical information, we cannot demonstrate this hypothesis. Nevertheless, if we restrict attention to the sample of optically well characterized single G stars, we find that the M_v distributions for the corresponding optical and X-ray samples cannot be distinguished even at the 49% level.

III. DATA REDUCTION

a) Source Detection

The X-ray data were obtained with the imaging proportional counter (IPC; Gorenstein, Harnden, and Fabricant 1981) on board the *Einstein Observatory* (Giacconi *et al.* 1979). Because uniform data reduction is not less important than homogeneity of the star sample, we have employed the local background detection algorithm of the finalized standard processing software (Harnden *et al.* 1984). This allowed homogeneous determination of count rates or upper limits for all potential X-ray sources. The processing software searches for X-ray sources in three different bands: soft (0.16–0.8 keV), hard (0.8–3.5 keV), and broad (0.16–3.5 keV) within a detection cell whose size depends on the band.[4] For the detected X-ray sources presented here, the statistical significance is such that the probability of a spurious detection due to a statistical background fluctuation at the position of one of our survey stars is $\sim 5 \times 10^{-3}$. By considering the number of detection cells occupied by our survey stars in the 66 IPC sequences examined, we estimate the number of spurious detections reported here to be ~ 0.3.

b) Source Strength

Corrections must be made for three instrumental effects: (1) the dependence of the IPC sensitivity on the source position within the $1° \times 1°$ field of view (e.g., vignetting), (2) the mirror point response function, and (3) the width of the IPC point response function (PRF). The standard processing thus applies three distinct correction factors in computing the "true" count rate from the measured number of source counts (see Harnden *et al.* 1984). However, both the mirror response and the IPC PRF corrections are dependent on the assumed source spectrum; furthermore, due to the size of the broad-band detection cell and the relatively soft stellar spectra, $\sim 50\%$ of the stellar source counts fall outside the broad detection cell. We have corrected for the latter effect by collecting net source counts in a circle of 3′ radius centered at the source position, so that essentially all the source counts are properly collected. For stars in our sample which are not detected as X-ray sources, the processing computes the 3 σ upper limits in the broad-band detection cell centered on the optical position; again, we modify the measured values using a derived correction factor based on comparison of count rates in the broad-band detection cell and in our 3′ circle for the detected stars. The statistical error on the upper limits turns out to be of the same order of magnitude as the estimated statistical error on this correction, which is $\sim 25\%$, comparable to the intrinsic statistical error on the detected source count rates.

We use a conversion factor of 2×10^{-11} in order to convert IPC count rates to apparent fluxes in the energy range 0.15–4.0 keV, which has been computed assuming a thermal spectrum (continuum + lines) from a plasma with solar abundances at a temperature $\log T = 6.5$. This temperature is rather typical for many of the sources for which preliminary spectral analysis has been performed (Schmitt *et al.* 1985*b*; Majer *et al.* 1986). Moreover, Schmitt *et al.* (1985*a*) show that the conversion factor will change less than a factor of 2 in the temperature interval $\log T = 6.25$–7.0 in the chosen energy band.

The derived values for the X-ray fluxes are summarized in Table 2. Taking into account the $\sim 50\%$ error in the conversion factor, i.e., in the assumed spectrum, and the $\sim 25\%$ intrinsic error in the measured source count rate, we estimate an overall error of 60% or less for all the quoted fluxes. Finally, we have also computed the value (or the upper limit) for the X-ray luminosity for each star; because the individual distances are known only to within an error of 20% or less, we estimate an overall error of 0.25 in the logarithm of the X-ray luminosity. The derived values for the X-ray luminosity are summarized, together with other relevant data, in Table 3.

IV. RESULTS

In this section, we discuss the statistical properties of the sample of stars considered here, and consider the consequences for models of stellar activity. In order to properly describe the statistical attributes of the data in hand, we took full advantage of recently developed techniques to compute maximum likelihood distribution functions of the censored data. This allowed us to take into account both measurements and upper/lower limits (Avni *et al.* 1980; Avni and Tananbaum 1982; Schmitt 1985), both in the evaluation of the range of values of individual stellar properties and in the correlation of distinct stellar properties.

a) The dG *Star X-Ray Luminosity Function*

The integral X-ray distribution function for our sample of single dG stars is shown in Figure 3*a*. From this distribution, we find that

$$\langle \log L_x \rangle = 27.4 \pm 0.2$$

and

$$\log L_x^{\rm median} = 27.0 \pm 0.3 ,$$

where the luminosities are in units of ergs $\mathrm{s^{-1}}$, and the quoted 68% confidence level uncertainties are derived from bootstrap calculations (Efron 1982; Schmitt 1985) of both the mean and the median. Since a large percentage of the observations are pointed exposures, we verified that our sample is not biased toward more active (i.e., more interesting) stars: in fact, the values of $\langle \log L_x \rangle$ and ($\log L_x^{\rm median}$) for the subsample of all pointed stars do not differ from the corresponding values for a similar subdivision of the single stars only.

For comparison, we also show in Figure 3*b* the integral X-ray luminosity functions for single dF stars in the range $0.3 \leq B-V \leq 0.5$ (Schmitt *et al.* 1985*a*) and for single dM stars with spectral type earlier than M5 within 25 pc (Rosner, Golub, and Vaiana 1985). Although the mean X-ray luminosity of single dM stars is quite similar to the corresponding mean value for the single dG stars (as expected from the results

[4] The detection cell is 2.′4 × 2.′4 in the broad and hard energy bands; in the soft band, the detection cell is 4′ × 4′.

TABLE 2

X-RAY FLUXES (0.15–4.0 keV) OF THE SAMPLE STARS

Star Name	Multiplicity[a]	Sequence Number	f_x[b] (10^{-13} ergs s^{-1} cm^{-2})	f_x[c] (10^{-13} ergs s^{-1} cm^{-2})	Remarks
W17	S	5430	...	<2.93	
W9012	S	7958	...	9.52	
W34A	S	2246	5.36	1.23	77% or X-ray emission can be attributed to 34B (dM0) on the basis of HRI observation (Harris and Johnson 1985)
W9032	S	5988	...	3.64	
W9035	S	7326	...	<1.07	
W71	M	3104	...	<3.86	
W9073AB	M	5697	...	<5.10	
W9085	S	7922	...	<1.25	
W9092AB	M	7894	...	<1.92	
W9095	M	5181	...	2.05	
W124	S	4418	...	1.29	
W137	S	7955	...	52.85	
W139	S	3105	...	<2.33	
W147	S	3152 4496	<1.01 <3.41	<1.01	
W160	M	7918	...	17.65	
W9177	S	7705	...	<6.19	
W202	M	4348	...	80.47	
W209	S	5480	...	<2.29	
W222	M	4347	...	77.64	
W9205	S	6704 7197	<2.61 <2.85	<2.61	
W9209	M	4931	...	<1.17	
W291	M	10669	...	1.28	
W311	S	501 4456 6964	48.69 53.13 48.22	50.01	Mean value adopted
W327	S	7954	...	10.10	
W9286	M	5186	...	<5.89	
W364	S	5516	...	<0.58	
W368	S	5985	...	<1.63	
W9322	S	6681	...	<2.38	
W384A	M	4135	...	2.30	
W395	M	5527	...	17.40	
W417	M	3122	...	10.03	
W9357	S	148	...	<9.19	
W434	S	3530	...	27.63	
W449	M	4455	...	17.23	
GJ 1152	S	4605	...	<2.11	Upper limit due to source confusion
W475	M	3929	...	2.44	
W502	M	4457	...	19.55	
W504	M	3531	...	49.64	
W534	M	851	...	7.49	
W547	S	4145	...	<1.55	
W559A	S	4436	153.7	46.11	70% of X-Ray emission can be attributed to W559B (K0 V) on the basis of HRI observation (Golub *et al.* 1982)
W561	S	5565	...	<2.06	
W584AB	M	1040	...	4.42	
W598	M	5576	...	2.33	
W9537	M	3986 4264	3.62 2.66	3.14	Mean value adopted
W9538	M	5191	...	47.37	
W9542	M	161	...	<2.09	
W9583	S	5992	...	13.12	
W666AB	M	5597	...	<1.38	
W672	M	9017	...	<1.36	
W684AB	M	10103	...	17.29	
W695ABC	M	4422	...	<2.45	
W746	M	5196	...	<2.34	
W9658	S	3172	...	<2.61	
W780	S	3114	...	<4.79	
W779	M	7914	...	1.92	
W9685	M	5993	...	19.96	
W9751	S	7605	...	29.12	
W882	S	7961	...	<1.32	
W9812AB	S	337	...	<2.32	
W904	M	5666	...	3.96	

[a] We consider a source (or upper limit) to be multiple (M) (for purposes of determining X-ray fluxes) if there is at least one other optical source within a 2′ radius of the optical counterpart of the IPC source and as long as there is no additional X-ray information from HRI exposures which resolves the sources; single (S) otherwise.

[b] X-ray fluxes from multiple IPC exposures of the same star or from single IPC exposures whence an HRI exposure is also available.

[c] Adopted X-ray fluxes.

TABLE 3

X-Ray Luminosities, Ages, and Rotational Velocities

Star Name	Log L_X (0.15–4.0 keV)	t (10^9 yr)	Reference	$v \sin i$ (km s^{-1})	Reference	V_{eq} (km s^{-1})	Reference
Sun	27.30	4.6	1	1.9 ± 0.3	1	2.0	2
W17	<27.26	...		...		...	
W9012	28.68	0.9	3	7.0 ± 0.8	1	6.4	4
W34A	26.70	>2.3	3	1.5 ± 0.8	1	...	
W9032	28.26	...		...		...	
W9035	<27.90	...		...		...	
W71	<26.78	...		2.2 ± 1.1	5	...	
W9073AB	<28.58	...		...		...	
W9085	<27.95	...		...		...	
W9092AB	<28.09	...		...		...	
W9095	28.19	...		...		...	
W124	27.32	1.9	3	3.5 ± 0.7	1	...	
W137	28.75	2.0	2	...		5.1	4
W139	<27.03	...		...		...	
W147	<27.51	2.0	3	4.5 ± 1.0	1	...	
W160	28.65	1.1	3	3.0 ± 0.7	1	...	
W9177	<28.67	...		...		...	
W202	29.38	0.2	3	15.0	6	...	
W209	<27.94	...		...		...	
W222	28.95	0.6	3	9.4 ± 0.4	1	10.1	2
W9205	<28.23	...		...		...	
W9209	<27.90	...		...		...	
W291	27.56	2.1	3	...		...	
W311	29.10	0.4	3	9.5 ± 0.6	1	...	
W327	28.22	>2.6	3	≤6.0	6	...	
W9286	<28.60	...		...		...	
W364	<27.04	2.6	3	...		...	
W368	<27.65	>2.7	3	1.8 ± 0.8	1	...	
W9322	<28.19	...		...		...	
W384A	27.80	...		...		...	
W395	28.55	4.3	3	≤6.0	6	...	
W417	28.83	1.1	3	4.5 ± 0.8	1	6.8	4
W9357	<28.58	...		...		...	
W434	28.35	...		...		2.7	4
W449	28.32	>8.0	3	4.0 ± 0.8	1	...	
GJ 1152	<28.10	...		...		...	
W475	27.39	>3.9	3	1.8 ± 0.8	1	...	
W502	28.21	2.1	3	4.3 ± 0.6	1	4.3	4
W504	29.00	0.1	3	7.7 ± 0.6	1	...	
W534	27.94	...		...		...	
W547	<27.70	>1.6	3	1.0 ± 10	1	...	
W559A	26.99	...		5.0	5	1.0	7
W561	<27.96	...		...		...	
W584AB	28.15	0.6	3	2.8 ± 0.7	1	...	
W598	27.50	>3.5	3	2.4 ± 0.8	1	2.9	2
W9537	28.33	>3.2	1	1.5 ± 0.5	1	...	
W9538	29.43	...		...		...	
W9542	<27.95	...		...		...	
W9583	28.82	1.2	3	5.5 ± 0.7	1	7.1	4
W666AB	<26.98	...		...		...	
W672	<27.48	>2.2	3	1.5 ± 0.5	1...		
W684AB	28.65	1.1	3	4.3 ± 0.8	1	...	
W695ABC	<27.25	...		...		...	
W746	<27.91	...		...		...	
W9658	<28.11	...		...		...	
W780	<27.27	...		...		...	
W779	27.83	2.5	3	3–5	6	3.8	4
W9685	29.09	...		...		...	
W9751	28.90	0.5	3	10.2 ± 1.1	1	11.4	4
W882	<27.47	>3.2	1	1.7 ± 0.8	1	...	
W9812AB	<28.24	...		...		...	
W904	27.98	4.0	3	5.7 ± 0.7	1	...	

References.—(1) Soderblom 1982. (2) Noyes *et al.* 1984. (3) Duncan 1981. (4) Baliunas *et al.* 1983. (5) Smith 1979. (6) Kraft 1956. (7) Hallam and Wolff 1981.

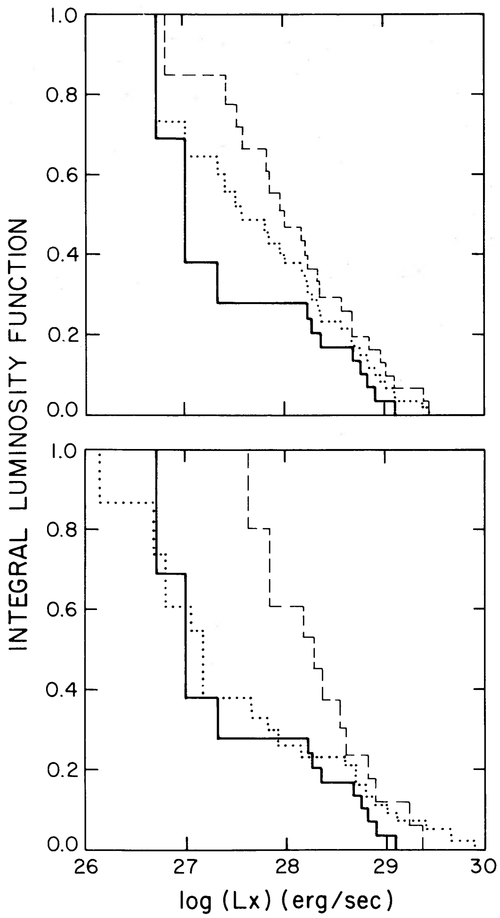

FIG. 3.—(*a*) Integral X-rays luminosity functions for single stars (*solid*), multiple stars (*dashed*), and total sample (*dotted*). (*b*) Comparison for integral X-ray luminosity functions for single F7–G9 stars (*solid*), single F stars with $0.50 \leq B-V \leq 0.30$, within 30 pc (from 1985) (*dashed*), and single dM stars earlier than M5 and within 25 pc (from Rosner, Golub, and Vaiana 1985) (*dotted*).

of the early stellar surveys, e.g., Vaiana *et al.* 1981), the range of luminosities for the dM stars is about four orders of magnitude, and thus approximately one order of magnitude broader than the luminosity range for the dG stars (see, however, the M-dwarf X-ray luminosity function given by Caillault *et al.* 1986, which is based on an X-ray selected sample). In contrast, the X-ray luminosity function for dF stars is about one order of magnitude narrower than the corresponding dG distribution.

b) *X-Ray Luminosity and Color*

In Figure 4 we show the scatter diagram of X-ray luminosity detections and upper limits versus $B-V$ color. A representative position for the Sun is also shown, with the range of expected solar luminosities between periods of minimum and maximum activity indicated by a vertical bar. The observed luminosities in our survey cover a range from $\log L_x = 26.7$ (Woolley 34A, G0 V) to $\log L_x = 29.43$ (Woolley 9538, F8 IV + unclassified companion). Although the apparent excess in the number of the upper limits with respect to detections at large values of $B-V$ might suggest a dependence of X-ray luminosity on stellar color, detailed study does not bear this out. Thus, we have performed linear regression of $\log L_x$ against $B-V$, taking into account both detections and upper limits, and using the detection levels of multiple systems as upper limits to the emission of the solar-like stellar component in each such multiple system. The result gives a correlation coefficient of -0.06, consistent with no correlation; furthermore, a bootstrap calculation of the correlation coefficient, using 200 replications (Efron 1982; Schmitt 1985), shows that the 68% confidence interval for the correlation coefficient (from -0.25 to 0.10) brackets zero. We conclude that there is no correlation between L_x and $B-V$ in our sample.

c) *Effects of Multiplicity*

As recently shown by Schmitt *et al.* (1985*a*), it is quite important to carefully distinguish between single stars and multiple systems and to treat them as independent samples: the presence of a companion which is optically faint does not exclude the possibility that this companion dominates the X-ray emission from the combined system. Hence, inclusion of such multiple sources in a sample of single stars in a given spectral range can lead to erroneous conclusions regarding the X-ray properties of single stars. We therefore considered sources to be multiple (as indicated by the key letter M in the second column of Table 2) if (1) there was at least one other optical star within a 2′ radius of the nominal optical counterpart of the IPC source (a limit imposed by the IPC angular resolution), and (2) there was no additional X-ray information from high resolution imager (HRI; cf. Giacconi *et al.* 1979) exposures which resolved the sources (in which case we considered them "single"). Only in one case (Woolley 9812) did we deviate from this procedure and attribute all of the system's X-ray emission to the secondary: in this isolated case, the secondary is a solar-like G2 V star, while the primary is an A2 source star whose contribution to the total X-ray emission is expected to be negligible (Schmitt *et al.* 1985*a*). These considerations lead to two distinct subsamples: (1) the single stars (11 detections and 19 upper limits), and (2) all multiple sources (21 detections and 10 upper limits).

Application of a Kolmogorov-Smirnov two-sample test based on values for the sensitivities derived from the local IPC background shows that the threshold distributions for the two subsamples (single and multiple sources) were in fact drawn

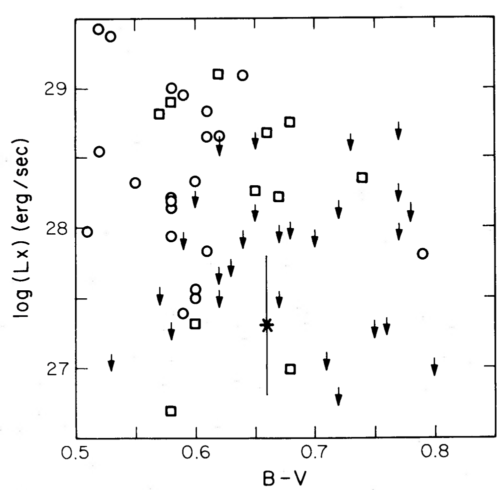

FIG. 4.—Scatter plot of X-ray luminosities (and upper limits) vs. $B-V$ color. *Squares*, detections of single stars; *circles*, detections of multiple stars; *downward arrows*, upper limits regardless of multiplicity. The asterisk represents the Sun; the luminosity variation over the solar cycle is also shown.

from the same parent distribution. This result allows us to compare the luminosity functions of single and all multiple sources by applying a two-sample Wilcoxon rank test (cf. Schmitt 1985). We find that the null hypothesis,

$$H_0: F_M(L_x) = F_S(L_x) ,$$

i.e., that the two samples of X-ray sources are drawn from the same parent population, can be rejected at the 98% (2.3 σ) confidence level (with a χ^2 of 5.03 with one degree of freedom).

The simplest explanation for this relatively weak result is to assume the presence of two (or more) unresolved X-ray emitters in systems which show multiple optical components. This working hypothesis can be tested by convolving the luminosity function of the single dG stars with itself (for the case of systems with components of similar spectral type), or with the luminosity function of the dM stars (from, e.g., Rosner, Golub, and Vaiana 1985) if the secondary is a star of later spectral type. The results of these convolutions are shown in Figure 5. Since the convolved distributions are virtually identical to the distribution of the multiple systems with dG primaries, our working hypothesis is supported.

d) Correlation of X-Ray Emission with Ca II *Emission*

The strikingly wide range of stellar X-ray emission for a given spectral type discussed above is also a general feature of other indicators of stellar activity, such as the Ca II H and K line intensity (Noyes *et al.* 1984; Rutten 1984; Soderblom 1985). This commonality is not surprising, since there is a general consensus that the phenomena of stellar activity share a common origin in the magnetic surface activity of late-type stars. To quantify this relationship, we have considered the correlation between X-ray luminosity and Ca II H–K emission (as parameterized by the Ca II R'_{HK} index). Using the Ca II data published by Noyes *et al.* (1984) and Soderblom (1985), we show in Figure 6 a scatter plot of log L_x versus log R'_{HK} for the stars in common in the X-ray and the Ca II samples. Linear regression to the data, including both detections and upper bounds, yields

$$\log L_x = 39.9 + 2.54 \log R'_{HK} ,$$

with a correlation coefficient of 0.84. Using bootstrap calculations, we obtain a 68% confidence limit interval of (0.77, 0.90) for this coefficient and thus can conclude that L_x and Ca II H and K emission are well correlated. This degree of correlation is in fact surprisingly good, considering that (1) by the solar analogy the activity-related emission levels are expected to vary substantially over the course of both the stellar magnetic cycle and a stellar rotation, and (2) the values of L_x are instantaneous measurements, whereas the values of R'_{HK} are means computed over long intervals of time ($\sim$20 yr).

We note that R'_{HK} measures the intensity of the line corrected for the contribution of the photospheric continuum and scaled for the bolometric flux; in the spectral range we cover, the bolometric luminosity changes only by half an order of magnitude, while the observed range of variation for L_x is about three orders of magnitude. Hence the correlation found above is not likely to be vitiated by further corrections to the Ca II flux index.

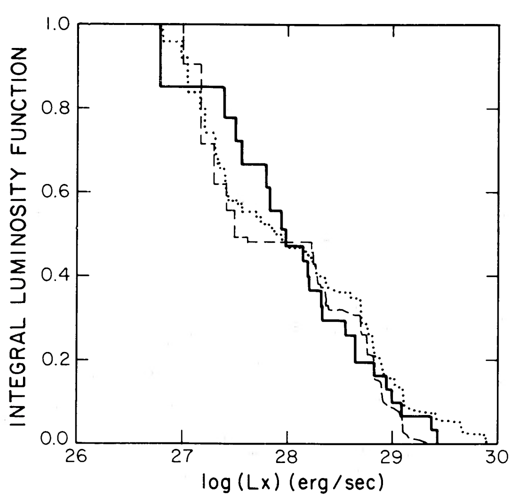

FIG. 5.—Integral X-ray luminosity functions for multiple F7–G9 stars (*solid*) and for the convolutions of the single F7–G9 star distribution function with itself (*dashed*) and with the single dM star distribution function (*dotted*) (from Rosner, Golub, and Vaiana 1985).

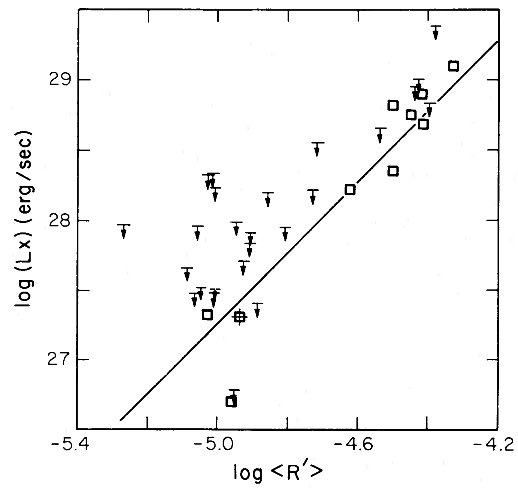

FIG. 6.—Scatter plot of X-ray luminosity and upper limits vs. the Ca II R'_{HK} emission index (from Noyes *et al.* 1984 and Soderblom 1985). The best-fit power-law relation is also shown; this fit assumes that all multiple stars (detected or not) are upper limits. The X-ray detected single stars are indicated by squares and the boxed plus represents the Sun.

e) Correlation with Rotation

The above-discussed correlation between L_x and R'_{HK} suggests a common origin for the plasma heating which must lead to these radiative emissions, i.e., one would expect a link between the energy release processes in the chromospheres and coronae of the observed sources. We know that the heating of the atmospheric gas layers above the photosphere is nonthermal in nature and is strongly related to the presence of magnetic fields. Because the generation of these magnetic fields is commonly viewed as a consequence of a magnetic dynamo functioning in the interior of a late-type dwarf star, and hence is expected to be related to the rotational state of the star, it is natural to look for a relationship between the X-ray emission and the stellar surface rotation velocity. Such a relationship has been long known for the general class of late-type stars (e.g., Pallavicini *et al.* 1981; Walter 1981, 1982), and more specifically for stars with spectral type later than $B-V \geq 0.3$ (Schmitt *et al.* 1985*a*; see also Walter 1983).

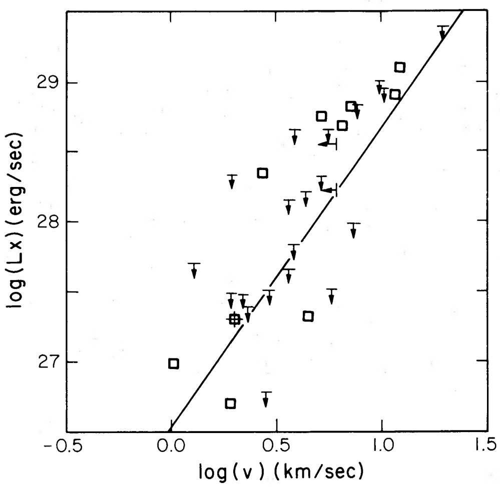

FIG. 7.—Scatter plot of X-ray luminosity vs. rotational velocity. Square, single stars. The indicated best-fit power-law relation again assumes that all the multiple stars (detected or not) are upper limits.

In order to quantify the relationship between X-ray luminosity and stellar rotation rate for our sample of stars, we have plotted in Figure 7 the values of L_x for sources from our survey against their rotation rate ($v \sin i$ or v_{eq}, taken from the literature as noted). For the present purpose, we regard the X-ray luminosity data for the unresolved detected multiple systems as upper bounds to the intrinsic X-ray luminosity of the dG component. The question we are addressing is then whether the regression laws previously found for dF stars, and for the entire range of late-type dwarf stars, also hold for the spectral type range we consider here.

Linear regression was performed for the $\log L_x$–$\log v$ data shown in Figure 7. Rotational velocities were computed from the available periods or from $v \sin i$ values (see Table 3 for references) statistically corrected by the factor $\langle \sin i \rangle = \pi/4$ (Chandrasekhar and Munch 1950); values of radii are from Allen (1976). We note that for α Cen (Woolley 559) we prefer the tentative value for the period obtained by Hallam and Wolff (1981) from UV observations. The best-fit power law we obtain is

$$\log L_x = 2.1 \log v + 26.5 ,$$

with a correlation coefficient of +0.79 (and a 68% confidence interval for this coefficient of 0.70–0.86); the corresponding 68% confidence interval for the slope of this relation spans from 1.7 to 2.7.

Our result is in good agreement with the corresponding relation found by Pallavicini *et al.* (1981), who studied a wide color range of stars (from dF7 through dM5). This suggests that this relation is relatively independent of the spectral type range considered, at least within the uncertainties imposed by our ignorance of the stellar spin axis orientations and by the above-mentioned intrinsic variability.

f) *Correlation with Rossby Number*

The dynamo efficiency, and hence the X-ray activity level, is also expected to be influenced by the properties of the convection zone. In this connection, it has been shown that the intensity of Ca II lines is related to the Rossby number (Noyes *et al.* 1984), and similarly to the level of X-ray emission (cf. Vilhu 1984; Schmitt *et al.* 1985*a*; Micela, Sciortino, and Serio 1985). As is well known, the Rossby number R_0 ($\equiv P/\tau_c$, where P is the stellar rotation period, and τ_c is the convective eddy turnover time scale at the base of the convection zone) is a measure of the effect of rotation on the dynamics of overturning eddies (and hence a measure of the influence of the "α-effect" in the magnetic dynamo, note that R_0 scales as the inverse square root of the dynamo number in linear theory; see below, and also Durney and Latour 1978). More specifically, Noyes *et al.* (1984) showed that nonthermal Ca II H–K line emission at chromospheric level, scaled by the bolometric flux, is well correlated with the Rossby number. Schmitt *et al* (1985*a*) showed further that a correlation of the form $L_x \propto R_0^{-2}$ holds at least for early F stars with $B-V \gtrsim 0.3$. Moreover, they suggested that such a law could account for the relation $L_X \propto (v \sin i)^2$ found by Pallavicini *et al.* (1981); this is easily seen by noting that

$$R_0 = \frac{P}{\tau_c} = \frac{2\pi R}{v\tau_c} = \frac{1}{v} f(B-V) ,$$

where R is the stellar radius and v is the equatorial rotation speed. Hence, since $L_X \propto R_0^{-2}$, we have immediately

$$\log L_x \propto \log v^2 + \log [f(B-V)]^{-2} ,$$

where $f(B-V)$ is a term describing how R_0 and τ_c depend on the $B-V$ color, and hence how R_0 changes with the spectral type of the source (for fixed rotational velocity). Because we have available rotational data only for a restricted color range, namely $0.51 \leq B-V \leq 0.74$, so that the actual variation of $f(B-V)$ is $\sim 1/10$ the observed variation of rotation rates, we do not expect our results to be strongly influenced by the color dependence of R_0.

In order to compute the convective turnover time τ_c, and hence R_0, we used the empirical relation given by Noyes *et al.* (1984), which was adjusted to match the chromospheric data from their survey. We show the scatter plot of $\log L_x$ versus log R_0 for our sample in Figure 8; assuming a simple power-law

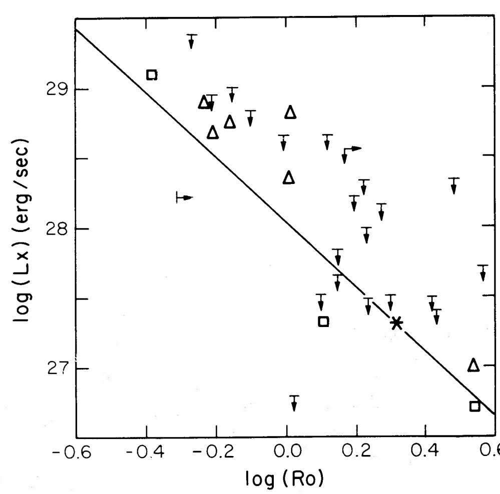

FIG. 8.—Scatter plot of X-ray luminosity vs. Rossby number. Triangles, X-ray detected stars with a known period of rotation; *squares*, detection of single sources with only $v \sin i$ values available. The Sun is also indicated by an asterisk. The best-fit power-law relation again treats all the multiple stars as upper limits.

relation, we find as the best fit

$$\log L_x = -2.3 \log R_0 + 28.0 ,$$

with a correlation coefficient $r = 0.80$ (and a 68% confidence level interval of 0.72–0.90; the corresponding confidence level interval for the slope of the power law is 2.1–2.6).

It is fair to ask at this point whether this correlation between the level of activity and the Rossby number is physically plausible. On the superficial level, one would expect a correlation between the level of activity and the dynamo number N_d (which is an essential parameter in linear theory). Now, recall that (Parker 1979)

$$N_d = \alpha(\nabla_r \Omega)d^4/\eta^2 ,$$

where α is the product of the mean helicity $\langle \boldsymbol{v} \cdot \nabla \times \boldsymbol{v} \rangle$ and the characteristic convective turnover time τ_c at the base of the convection zone, $\nabla_r \Omega$ is the radial gradient of the angular velocity Ω, d is the characteristic scale length of convection (e.g., the typical eddy scale size at the base of the convection zone), and η is the turbulent magnetic diffusivity. If we assume that $\nabla_r \Omega$ scales as Ω/d, then we in fact recover the relation $N_d \propto R_0^{-2}$. It is not obvious why one would obtain this required scaling of the differential rotation rate (because one would expect it to depend on the details of the spindown process and on the history of spindown of a given star), but this line of reasoning does suggest that the scaling of the activity level on the properties of the interior rotation can act as a probe for the stellar spindown process.

g) Correlation with Age

Any theory which seeks to explain the properties of X-ray emission throughout the H-R diagram must also account for the evolution of this emission as the stars "age." That the level of X-ray emission ought to vary with stellar age follows from the fact that stars lose angular momentum in the course of their evolution and from the observed correlation of L_x with rotation. Moreover, because it has been shown (from studies of open clusters) that the decay of the X-ray luminosity level with age is spectral type–dependent (Micela *et al.* 1985), it is worthwhile to consider each spectral type separately.

By considering the "local" population of the solar-like stars as a group, with a mean age of $\sim 3 \times 10^9$ years, we have compared its X-ray luminosity distribution function with the analogous X-ray luminosity distribution functions for the solar-like stars of the Hyades cluster (Stern *et al.* 1981; age $\sim 6 \times 10^8$ yr), th solar-like stars of the Pleiades cluster (Micela *et al.* 1985; age $\sim 5 \times 10^7$ yr), and the G stars of Orion Ic cluster (Smith, Pravdo, and Ku 1983; age $\sim 2 \times 10^6$ yr). In this lattermost sample, we considered only sources with $v \sin i \lesssim 25$ km s^{-1} because faster rotators may be more massive and will contract on the main sequence as A or early F stars (see discussion in Smith, Pravdo, and Ku 1983). The correspoding four luminosity functions are shown in Figure 9*a*, where a trend of decreasing luminosity with increasing stellar age is evident. This result is made clearer if we compute the mean values of the X-ray luminosity for each of the four distributions we are considering and plot them against mean stellar age. The result is shown in Figure 9*b* and clearly indicates the strong dependence of stellar activity level on stellar age. Because of the mixing of young and old disk population stars, the local population is quite inhomogeneous with respect to stellar age; in order to correct for this effect, we have also investigated the correlation between the level of X-ray luminosity and individual stellar age, as computed from the observed Li abundance (Duncan 1981; Soderblom 1983). The result of this analysis is shown in Figure 9*c*, a log-log scatter plot of X-ray luminosity versus age for those stars for which we have Li age determinations. The clear correlation between the level of X-ray emission and the stellar age as determined from the Li abundance is a striking feature of this plot.

Although a number of authors have explored a variety of functional forms for the dependence of stellar activity indicators on stellar age (cf. Vilhu 1984, Catalano and Marilli 1983; Duncan 1981; Simon, Herbig, and Boesgaard 1985), we have not pursued this issue because the data in hand do not warrant such detailed modeling. Instead, we have confined attention to the simplest relation, namely a power law of the form

$$L_x = At^{-\alpha} .$$

Using linear regression analysis in log space, we have obtained the most probable values for the coefficients A and α,

$$\log A \approx 42.1^{+2.7}_{-2.0} ,$$

$$\alpha \approx 1.5^{+0.3}_{-0.2} ,$$

with a correlation coefficient $r \approx 0.77^{+0.08}_{-0.09}$. In all cases, the uncertainties given are the 68% confidence level intervals derived by bootstrapping (using 200 replications). As discussed above, this analysis includes the sample of the single stars, including both detections and upper limits in L_x, as well as all lower bounds for stellar age; as above, we have also included the data for the multiple systems, whose X-ray luminosities are treated as upper bounds to the intrinsic X-ray luminosities of the dG component.

An interesting aspect of this analysis is brought out by comparing our results with those of Simon, Herbig, and Boesgaard (1985), who considered a similar sample of stars in an analysis of chromospheric and transition region line emission versus stellar age. Simon *et al.* have shown that, independent of the functional form of the relation connecting the activity indicator with stellar age, the decay time of the total line luminosity decreases with the temperature of line formation, e.g., with the height of the atmospheric layer in which the line of interest is formed. Our results indeed confirm this trend in the sense that the *e*-folding decay time derived from our X-ray sample is $\sim 1.1 \times 10^9$ yr, as would be expected from naive extrapolation of the results of Simon *et al.* In order to confirm that our sample is indeed consistent with theirs, we have also tested for the Ca II H–K line intensity correlation with stellar age for our sample; as shown in Figure 9*d* (which displays the corresponding scatter plot for our data sample), the power-law dependence of the R'_{HK} parameter on stellar age we derive is in agreement with that found by Simon *et al.* (with statistical errors).

V. SUMMARY

Using a volume-limited sample of late F and G dwarf stars, we have investigated the properties of coronal X-ray emission from solar-type stars. Our principal results may be summarized as follows:

a) Our sample of stars is representative of the local population of main-sequence sources within 25 pc.

b) The X-ray luminosity functions of sources in our survey with single- and multiple-component optical counterparts differ at the 98% confidence level; this difference can be simply explained by assuming that sources with multiple optical com-

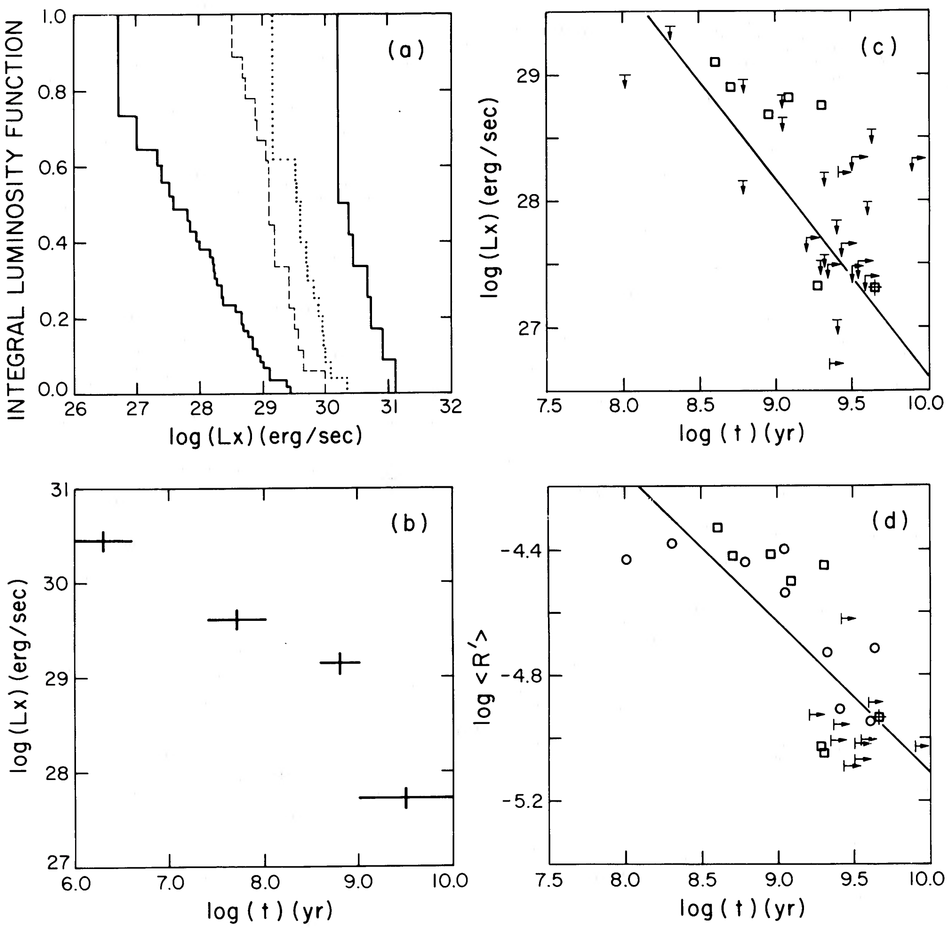

FIG. 9.—(*a*) Integral X-ray luminosity functions for (*left to right*) the nearby dG stars (this survey), dG Hyades cluster members (from Stern *et al.* 1981), dG Pleiades cluster members (from Micela *et al.* 1985), and the slow-rotating dG stars of Orion Ic (from Smith, Pravdo, and Ku 1983). (*b*) Mean X-ray luminosities of the G stars in the above clusters and of the stars in the present sample vs. their mean age. (*c*) log-log scatter plot of X-ray luminosity and stellar lithium age. Single detected stars are indicated by squares. Also shown the best-fit power-law relation, obtained as in the earlier figures. (*d*) Scatter plot of the $R'_{\rm HK}$ index of chromospheric emission vs. stellar lithium age. Squares, single stars; *circles*, those stars considered multiple systems in our survey. *Solid line* best-fit power-law relation.

ponents consist of at least two unresolved X-ray emitters per X-ray source, with the optical secondary either a dG or later spectral type main-sequence star.

c) The strengths of activity indicated by radiative emission levels at two very distinct heights in stellar atmospheres, namely the corona (measured by the stellar X-ray luminosity) and the chromosphere (measured by the stellar Ca II H–K emission), are well correlated, supporting the common supposition that the activity at these distinct heights in stellar atmospheres have a common origin.

d) Linear regression applied to our data confirms the earlier finding of a power-law relation between the X-ray luminosity L_x and the projected equatorial surface rotation rate (Pallavicini *et al.* 1981).

e) Our data show a correlation between the X-ray luminosity L_x and the Rossby number R_0 similar to that found earlier by Schmitt *et al.* (1985*a*) for dF stars. As discussed by Noyes *et al.* (1984), this kind of correlation supports the contention that the observed activity is in large part the result of magnetic field generation in the convective interior of these stars.

f) Using data from our sample of dG stars in the field, together with data on similar spectral type stars in open clusters spanning a wide range of ages, we find that both chromospheric and coronal emission from stars in this spectral type range show a clear decrease of intensity with advancing age. This dependence is seen both by comparing the mean properties of field stars and clusters with their mean ages, and by comparing the X-ray (or Ca II H–K) emission level with the "lithium age" for individual stars in the total sample. While the Ca II H–K emission shows the well-known inverse square root dependence on age (cf. Skumanich 1972), the X-ray emission levels fall off faster, viz., as $t^{-3/2}$.

We would like to thank the Italian CNR, the Smithsonian Astrophysical Observatory, and NASA grants NAGW-112 and NAG8-445 and NASA contract NAS8-30751 for partial support of this work.

REFERENCES

Allen, C. W. 1976, *Astrophysical Quantities* (3d ed., London: Athlone).
Avni, Y., Soltan, A., Tananbaum, H., and Zamorani, G. 1980, *Ap. J.*, **238**, 800.
Avni, Y., and Tananbaum, H. 1982, *Ap. J.* (*Letters*), **262**, L17.
Baliunas, S. L., *et al.* 1983, *Ap. J.*, **275**, 752.
Basri, G., Laurent, R., and Walter, F. 1983, in *IAU Symposium 102, Solar and Stellar Magnetic Fields: Origins and Coronal Effects*, ed. J. Stenflo (Dordrecht: Reidel), p. 199.
Bookbinder, J. 1985, Ph.D. thesis, Harvard University.

Caillault, J., and Helfand, D. J. 1985, *Ap. J.*, **289**, 279.
Caillault, J., Helfand, D. J., Nousek, J. A., and Takalo, L. O. 1986, *Ap. J.*, **304**, 318.
Catalano, S., and Marilli, E. 1983, *Astr. Ap.*, **121**, 190.
Chandrasekhar, S., and Munch, G. 1950, *Ap. J.*, **111**, 142.
Duncan, D. K. 1981, *Ap. J.*, **248**, 651.
Durney, B. R., and Latour, J. 1978, *Geophys. Ap. Fluid Dyn.*, **9**, 241.
Efron, B. 1982, *The Jacknife, the Bootstrap and Other Resampling Plans* (Philadelphia: SIAM).
Eker, Z. 1985, preprint.
Giacconi, R. *et al.* 1979, *Ap. J.*, **230**, 540.
Gliese, W. 1969, *Catalogue of Nearby Stars* (Veröffentlichungen des Astronomishen Rechen-Instituts, University of Heidelberg, Vol. 22).
Gliese, W., and Jahreiss, H. 1979, *Astr. Ap. Suppl.*, **38**, 423.
Golub, L. 1982, in *Second Cambridge Workshop on Cool Stars, Stellar Systems and the Sun* ed. M. S. Giampapa and L. Golub (*Smithsonian Ap. Obs. Spec. Rept.*, No. 392), Vol. **1**, p. 39.
Golub, L., Harnden, F. R., Jr., Maxson, C. W., Rosner, R., R., Vaiana, G. S., Cash, W., and Snow, T. P. 1983, *Ap. J.*, **271**, 264.
Golub, L., Harnden, F. R., Jr., Pallavicini, R., Rosner, R., and Vaiana, G. S. 1982, *Ap. J.*, **253**, 242.
Gorenstein, P., Harnden, F. R., Jr., and Fabricant, D. G. 1981, *IEEE Trans*, **NS-28**, 869.
Hall, D. S. 1981, in *Solar Phenomena in Stars and Stellar Systems*, ed. R. Bonnet and A. K. Dupree (Dordrecht: Reidel), p. 431.
Hallam, K. L., and Wolff, C. L. 1981, *Ap. J. (Letters)*, **248**, L73.
Harnden, F. R., Jr., Fabricant, D. G., Harris, D. E., and Schwarz, J. 1984, *Smithsonian Ap. Obs. Spec. Rept.*, No. 393.
Harris, D. E., and Johnson, H. M. 1985, *Ap. J.*, **294**, 649.
Helfand, D. J., and Caillault, J. 1982, *Ap. J.*, **253**, 760.
Hoffleit, D., and Jaschek, C. 1982, *The Bright Star Catalogue* (New Haven: Yale University).
Johnson, H. M. 1983, *Ap. J.*, **273**, 702.
Kraft, R. P. 1967, *Ap. J.*, **150**, 552.
Majer, P., Schmitt, J. H. M. M., Golub, L., Harnden, F. R., and Rosner, R. 1986, *Ap. J.*, **300**, 360.
Micela, G., Sciortino, S., Serio, S. 1985, in *X-Ray Astronomy '84*, ed. M. Oda and R. Giacconi (Tokyo: Institute of Space and Astronomical Science), p. 43.
Micela, G., Sciortino, S., Serio, S., Vaiana, G. S., Bookbinder, J., Golub, L., Harnden, Jr., F. R., and Rosner, R. 1985, *Ap. J.*, **292**, 172.
Micela, G., Sciortino, S., Vaiana, G. S., Schmitt, J. H. M. M., Stern, R., Harnden, F. R., Jr., and Rosner, R. 1987, *Ap. J.*, submitted.
Noyes, R. W., Hartmann, L. W., Baliunas, S. L., Duncan, D. K., and Vaughan, A. H. 1984, *Ap. J.*, **279**, 763.
Pallavicini, R., Golub, L., Rosner, R. R., Vaiana, G. S., Ayres, T., and Linsky, J. L. 1981, *Ap. J.*, **248**, 279.
Parker, E. N. 1979, *Cosmical Magnetic Fields* (Oxford: Clarendon).
Rosner, R. 1983, in *IAU Symposium 102, Solar and Stellar Magnetic Fields: Origins and Coronal Effects*, ed. J. Stenflo (Dordrecht: Reidel), p. 279.
Rosner, R., *et al.* 1981, *Ap. J. (Letters)*, **249**, L5.
Rosner, R., Golub, L., and Vaiana G. S. 1985, *Ann. Rev. Astr. Ap.*, **23**, 413.
Rutten, R. G. M. 1984, *Astr. Ap.*, **130**, 353.
Schmitt, J. H. M. M. 1985, *Ap. J.*, **293**, 178.
Schmitt, J. H. M. M., Fink, G., and Harnden, F. R., Jr., 1986, in preparation.
Schmitt, J. H. M. M., Golub, L., Harnden, F. R., Jr., Maxson, C. W., Rosner, R., and Vaiana, G. S. 1985*a*, *Ap. J.*, **290**, 307.
Schmitt, J. H. M. M., Harnden, F. R., Jr., Peres, G., Rosner, R., and Serio, S. 1985*b*, *Ap. J.*, **288**, 751.
Simon, T., Herbig, G., and Boesgaard, A. M. 1985, *Ap. J.*, **293**, 551.
Skumanich, A. 1972, *Ap. J.*, **171**, 565.
Smith, M. A. 1979, *Pub. A.S.P.*, **91**, 737.
Smith, M. A., Pravdo, S. H., and Ku, W. H.-M. 1983, *Ap. J.*, **272**, 163.
Soderblom, D. R. 1982, *Ap. J.*, **263**, 239.
———. 1983, *Ap. J. Suppl.*, **53**, 1.
———. 1985, *A.J.*, **90**, 2103.
Stern, R. A., Zolcinski, M. C., Antiochos, S. C., and Underwood, J. M. 1981, *Ap. J.*, **249**, 647.
Topka, K. P., Avni, Y., Golub, L., Gorenstein, P., Harnden, F. R., Jr., Rosner, R., and Vaiana, G. S. 1982, *Ap. J.*, **259**, 677.
Vaiana, G. S. 1983, in *IAU Symposium 102, Solar and Stellar Magnetic Fields: Origin and Coronal Effects*, ed. J. Stenflo (Dordrecht: Reidel), p. 165.
Vaiana, G. S., *et al.*, 1981, *Ap. J.*, **245**, 163.
Vaiana, G. S., and Rosner, R. 1978, *Ann. Rev. Astr. Ap.*, **16**, 393.
Vilhu, O. 1984, *Astr. Ap.*, **133**, 117.
Walter, F. M. 1981, *Ap. J.*, **245**, 677.
———. 1982, *Ap. J.*, **254**. 745.
———. 1983, *Ap. J.*, **274**, 794.
Walter, F. M., Linsky, J. L., Simon, T., Golub, L., and Vaiana, G. S. 1984, *Ap. J.*, **281**, 815.
Wooley, R., Epps, E. A., Penston, M. J., and Pocock, S. B. 1970, *Royal Obs. Ann.*, Vol. **3**.

J. Bookbinder, L. Golub, F. R. Harnden, Jr., R. Rosner, and G. S. Vaiana: Harvard-Smithsonian Center for Astrophysics, 60 Garden Street, Cambridge, MA 02138

A. Maggio and S. Sciortino: Osservatorio Astronomico di Palermo, Palazzo dei Normanni, 90134 Palermo, Italy

P. Majer: Wroclaw Astronomical Observatory, ul. Kpernika 11, 51-622 Wroclaw, Poland